Robust Uneven Shift of Extreme Storm Surges Observed in Data Sparse Northeast Indian Ocean Cities

Md. Rezuanul Islam[1*], Htut Naing Thwin[2*], Hiroshi Takagi[2] and Yohei Sawada[1]

[1]Department of Civil Engineering, The University of Tokyo, Tokyo, Japan

[2]Department of Transdisciplinary Science and Engineering, Institute of Science Tokyo, Tokyo, Japan

Corresponding author: Md. Rezuanul Islam (fahiemislam@gmail.com)

*M. R. Islam and H. N. Thwin both have significantly contributed to the research

Key Points:

- Reanalysis based surge residual return levels for Northeast Indian Ocean (NIO) cities were evaluated with multi-model ensembles to quantify model selection uncertainty
- Statistical model choice strongly affects design surge levels, with the median of 50-year levels matching the median of 25-year levels under alternative tail assumptions
- Multi-model ensembles show the 1950 50-year surge becomes a 33- to 39-year event by 2000 in central NIO cities but less frequent in western cities

Abstract

Reanalysis-driven storm surge datasets enable extreme analysis in data-sparse regions, but most studies translate these time series into extremes using a single statistical model, leaving model-selection uncertainty unquantified. In this study, we analyze ERA5-forced surge residual dataset (1950–2024) from Copernicus Climate Change Service for 11 Northeast Indian Ocean (NIO) cities using an ensemble of nonstationary extreme value and Bayesian formulations to estimate return levels, implied return period changes in 2000 relative to 1950 baselines, and trends. Our multi-model ensemble analyses reveal that for inner NIO cities (e.g., South 24 Parganas, Patuakhali, Chittagong, Cox's Bazar)–near the head of the Bay of Bengal–the 1950's 50-year surge residual level (RL50) becomes more frequent by 2000 (typically a 33- to 39-year event corresponds to increase in median annual exceedance probability up to 51%), even though surge residual annual-maxima trends are negative (~ - 1 mm/year). These changes are not uniform across the NIO as several western NIO cities (e.g., Colombo, Chennai) show the opposite tendency, with longer implied return periods (typically a 66- to 104-year event) by 2000. Statistical model choice substantially affects design levels and their interpretation in areas with high storm surges. For example, Gumbel or Bayesian median estimates of RL50 can correspond to roughly a median of RL25 under Frechet tail assumptions for inner NIO cities, highlighting nontrivial structural uncertainty. Finally, we show that bias of High Resolution Model Intercomparison Project (HighResMIP)– ERA5 depends on the statistical model used to estimate return levels, and that an ensemble-of-models evaluation provides a conservative and transparent basis for benchmarking climate-model surge extremes against reanalysis.

Plain Language Summary

Coastal flooding from storm surges threatens many rapidly growing cities around the Northeast Indian Ocean (NIO), but long, high-quality tide gauge records needed to quantify rare extremes are often unavailable. Researchers therefore commonly rely on reanalysis-based storm surge datasets covering several decades. A key challenge is that translating these surge time series into design information, such as the surge level expected about once every 50-years, depends on the statistical method used. Most previous reanalysis-based studies adopt a single method which can hide uncertainty linked to model choice. We analyzed ERA5-based surge dataset spanning 1950 to 2024 for 11 NIO cities and combined several standard statistical approaches into an ensemble to capture model selection uncertainty. For central NIO cities, the 1 in 50-year event in 1950 became more frequent by 2000, occurring roughly once every 33-to 39-years, although annual maximum surges show a small long term decline. Several western and outer basin cities show the opposite tendency, with longer implied return periods by 2000. We also show that conclusions about how climate model simulations differ from reanalysis at design relevant extremes can change depending on the statistical method used. This work reflects the importance of ensemble analysis of reanalysis products that serve as reference baselines for evaluating climate-ensemble outputs and improving uncertainty aware assessment of present-day surge extremes in data sparse regions.

1 Introduction

Assessing long-term variability in extreme storm surges is critical for coastal risk management and adaptation planning (Islam, Duc, Sawada, et al., 2023; Wahl et al., 2017). Such information helps engineers and urban planners decide whether to protect, accommodate, and retreat from specific coastal areas (Islam et al., 2022; Hoshino et al., 2016). It also underpins the design of coast protection measures based on design-relevant surge heights (e.g., 50-year return level) for future planning horizons such as 2050 and 2100 (Kato & Tajima, 2023; Nimura et al., 2020). In particular, effective design of coastal defenses and resilient infrastructure depends on quantifying the extreme surge levels that are likely to be exceeded with a given probability, because these extremes drive flooding impacts and coastal erosion (Boettle et al., 2016). Extreme value theory (EVT) provides the statistical foundation for representing historical extremes with probability distributions and is widely used to estimate return levels and exceedance probabilities of storm surges (Coles, 2001). However, sparse and uneven in-situ observations—especially in many developing coastal regions—together with unquantified statistical model selection uncertainty, can hinder robust extremes analysis and yield overconfident or biased storm surge hazard estimates (Beck et al., 2020; Wahl et al., 2017).

In recent years, reanalysis-driven hydrodynamic products have advanced storm surge research by providing globally consistent tide-surge time series over many decades. Their coverage, consistency, and length enable analyses of extreme event footprints and spatial dependence (Enríquez et al., 2020; Li et al., 2023) and of climate influences on surge levels (Muis et al., 2023), beyond what single-site observations typically allow. Consequently, these datasets have been used to estimate exceedance probabilities, which are valuable input for coastal flood risk assessment for both disaster risk reductions and climate change mitigation and adaptation (Tiggeloven et al., 2020). Because these datasets are spatially coherent and regularly updated, they also serve as a common reference for benchmarking forecasts and climate model projections across institutions and regions (Dullaart et al., 2020; Vousdoukas et al., 2018). In data-sparse regions such as much of Asia and Africa, where long-term in-situ observations are scarce or absent, reanalysis-based products often represent the only feasible basis for investigating surge extremes (Aleksandrova et al., 2025; Muis et al., 2023). Consequently, they serve as a valuable resource for assisting coastal planners and risk practitioners. Nevertheless, reanalysis products (e.g., atmospheric, storm surge) are not free from limitations, including systematic regional biases and underestimation of extreme event intensities (Muis et al., 2016; Vousdoukas et al., 2018; Hersbach et al., 2020; Kosaka et al., 2024).

In much of the earlier reanalysis-based works, extreme surge statistics were derived using a single statistical model—so potential uncertainty in model choice remains largely unquantified even when physical reanalysis is carefully validated. For example, using the Global Tide and Surge Reanalysis, Muis et al. (2016) estimated return levels with a Gumbel fit to block maxima; in another study, Muis et al., (2020) used the Coastal Dataset for the Evaluation of Climate Impact and applied the same method to estimate return levels at a global scale. Vousdoukas et al., (2018) applied a transformed stationary extreme value methodology to reanalysis-driven storm surge data to estimate present-day surge return levels. These estimates served as the reference baseline against which climate-model-driven extreme sea-level (ESL) projections were compared, allowing the derivation of return levels and design allowances for coastal defense infrastructures

under future sea-level rise. Tadesse et al. (2022) analyzed five global storm surge time series from the Global Storm Surge Reconstructions database (Tadesse & Wahl, 2021) and assessed trends for 1980–2010 using a linear regression model. More recently, Copernicus Climate Change Service (2025) introduced a new global dataset of storm surges for 1950–2024, based on the ERA5 climate reanalysis and estimated extremes using Generalized Pareto Distribution (GPD). These real world estimates have further been used to validate their ensemble climate model-driven storm surge estimates. Together, these studies justify reanalysis as a practical reference for ESL estimation—but they also highlight that extreme value statistics (e.g., present day surge return level) are not free from uncertainty arising from the specific distributional choice. In this context, employing an ensemble of statistical models is essential for quantifying inter-model uncertainty, especially when reanalysis products serve as the reference baseline.

Multi-model ensemble is a standard practice in weather forecasting (e.g., Titley et al., 2019; Yamaguchi et al., 2015) and climate projection studies (Murphy et al., 2025; Cael et al., 2024; Chen et al., 2020) that enables explicit quantification of uncertainty and reduce the limitations inherent to individual model. Likewise, ensemble based storm surge forecasting (e.g., Flowerdew et al., 2013; Islam, Duc, & Sawada, 2023; Islam et al., 2026) and future projection studies (e.g., Shimura et al., 2022; Muis et al., 2023) has recently received considerable attention from the research community. However, uncertainties in reanalysis-based present-day storm surge estimates have not been assessed and hence have been ignored in all previous storm surge risk studies. Considering storm surge reanalysis as a reference baseline, interpreting extremes through multiple plausible statistical models can offer design-relevant estimates that are less sensitive to any single model assumptions and yield more reliable trends and return levels. For example, several prior studies (e.g., Wahl et al., 2017; Caruso & Marani, 2022; Baldan et al., 2022) demonstrated that statistical model choice can substantially alter high quantile estimates and yield significant spread in return levels from the same records of ESL. Consequently, adopting a multi-model ensemble framework can propagate structural differences into the predictive distribution, producing better uncertainty-informed return level intervals and reducing the risk of overconfident, single-model design guidance. Furthermore, multi-model ensembles can characterize bias more effectively than single-model summaries. For instance, Muis et al. (2023) compared global storm surge levels corresponding to 1, 10, and 100-year return period driven by an ensemble of climate models (1985–2014) against an ERA5-based baseline and reported spatially coherent biases—generally positive along semi-enclosed seas and negative in equatorial regions. Such bias diagnosis can be strengthened when the reference statistics are themselves multi-model ensemble-derived rather than single-model estimates, yielding more reliable bias quantification and greater confidence when interpreting climate model-driven outputs.

In this study, we leverage storm surge reanalysis to quantify present-day (1950–2024) storm surge return levels and trends by employing an ensemble of non-stationary standard statistical models. This approach is distinct from conventional practices that relies on a single statistical model to translate reanalysis time series into extremes. We apply statistical methods based on EVT and Bayesian formulations and explicitly account for model-selection uncertainty when estimating surge extremes for Northeast Indian Ocean (NIO) cities over 1950–2024. We also compare ensemble- and single-model-based present-day return levels with those derived from a climate model to strengthen bias diagnosis. Our analyses use the global dataset of storm

surges and ESL for 1950–2024 based on the ERA5 climate reanalysis together with High Resolution Model Intercomparison Project (HighResMIP) simulation outputs from Coupled Model Intercomparison Project Phase 6 (CMIP6; Copernicus Climate Change Service, 2025). This dataset represents the longest period and most comprehensive publicly available surge reanalysis to date. We focus on NIO cities not only because they host large vulnerable population (Becker et al., 2024; Takagi et al., 2023; Islam, 2025) but also because long-term in-situ surge records are scarce (Sprintall et al., 2024; Alamgir et al., 2025) and uncertainty-informed extreme surge estimate remains largely unexplored (Becker et al., 2024), making them an ideal test bed for a 75-year reanalysis. Overall, to our knowledge, this study is the first to demonstrate the value of multi-model statistical ensemble analysis of reanalysis-based surge products for evaluating climate-ensemble outputs and improving uncertainty aware assessment of present-day surge extremes in data-sparse NIO cities.

2 Materials and methods

Sea level data

We use recently released the global sea level change time series dataset which provides reanalysis- and climate model-forced hydrodynamic simulations of tides, storm surge residuals, mean sea level (MSL), and total water level from 1950 to 2050 (Copernicus Climate Change Service, 2025). The Deltares Global Tide and Surge Model (GTSM version 3.0) used to simulate sea level related variables using the meteorological forcing from ERA5 global reanalysis and an ensemble (5 member) of HighResMIP models from CMIP6. The grid resolution for hydrodynamic simulations ranges from 2.5 km along the coast to 25 km in the ocean and provides data at a 10-min temporal resolution. This dataset includes a global selection of coastal and ocean output points (virtual stations) of more than 43000. Aleksandrova et al. (2025) compared this reanalysis and in-situ total water level values at 262 observation stations globally and found a good overall agreement with a RMSE of 0.20 m and a Pearson correlations coefficient of 0.9. This 75-year long dataset represents the longest period and most comprehensive publicly available global sea level reanalysis to date. Further details including the model configuration, validation, and performance of the dataset can be found in Muis et al., (2023); Copernicus Climate Change Service (2025); Aleksandrova et al., (2025).

In this study, we specifically analyze historical (1950-2024) components of storm surge residual, defined as the difference between a total-water-level simulation (tide + meteorological forcing) and a tide-only simulation. Here, both simulations included spatially varying sea-level rise field. Because the surge is derived from two dynamically simulated water-level time series, non-linear interactions between tides, storm surges, and MSL are represented in the total-water-level run, while MSL changes are removed from the surge residual. Here, the storm surge reanalysis captures the meteorological non-tidal signal from both tropical-cyclone (TC) and non-TC conditions. However, “storm surge” is often used colloquially to denote TC forcing in cyclone-prone basins; here we use “surge residual” for the general component. In addition to ERA5- surge residual dataset, we also use Coupled Model Intercomparison Project Phase 6 High Resolution Model Intercomparison Project (HighResMIP)-forced surge residual and mean sea level (MSL) data. Both of these climate model outputs (surge residual and MSL) are co-located with the

reanalysis-based global surge residual outputs and available for the historical period of 1950-2014 (Copernicus Climate Change Service, 2025).

We extract reanalysis- and climate model-forced surge residual products for 11 major coastal cities (Fig. 1) in the NIO that span five countries and represent high exposure urban coastal settings (e.g., population density: >50,000 population/km^2): Colombo (Sri Lanka); Chennai, East Godavari, Jagatsinghapur and South Twenty-Four Parganas (hereafter S24 Parganas; India); Patuakhali, Chittagong and Cox's Bazar (Bangladesh), Sittwe and Yangon (Myanmar) and Mueang Phuket (Thailand). These cities are rapidly growing and contain critical infrastructures in low-lying deltas and estuaries that are highly exposed to coastal flooding. Several of these cities lie in TC-prone coastal zones where episodic surge extremes drive disproportionate impacts relative to mean conditions (Becker et al., 2024; M. R. Islam, 2025). Despite this vulnerability, long term in-situ sea level and surge observations remain sparse, discontinuous, or inaccessible across much of the region (Alamgir et al., 2025; Becker et al., 2024; Sprintall et al., 2024), limiting historically grounded extremes and trend analyses. Earlier global reanalysis-driven surge products (e.g., Muis et al., 2016, 2020) have also had limited utility for city-scale assessments across parts of the NIO, whereas the recently available global sea level change time series dataset (Copernicus Climate Change Service, 2025) offers consistent multi-decadal records with improved temporal and spatial coverage, motivating the present analysis.

To extract ERA5-surge residual time series (1950-2024), we selected virtual stations near each target city using administrative boundaries from the United Nations Office for the Coordination of Humanitarian Affairs (OCHA, 2025). For each city, we applied a 4-km coastal buffer around the administrative boundary to minimize boundary artifacts while retaining near-city coastal output points. We used multiple virtual stations per city rather than single point because coastal surge levels can vary substantially over short distances due to local bathymetry, coastline geometry and the placement of model nodes relative to channels/estuaries and open-coast segments. Sampling several nearby coastal output locations therefore provides a more representative characterization of city scale surge conditions and reduces the sensitivity to any single model node. In total, 60 virtual stations (hydrodynamic model output locations; point markers in Fig. 1) were selected and analyzed. A closer view of the virtual station locations for each city is provided in Supplementary Fig. S1. Summary statistics of the raw data are also included in the Supplementary Materials (Supplementary Fig. S2).

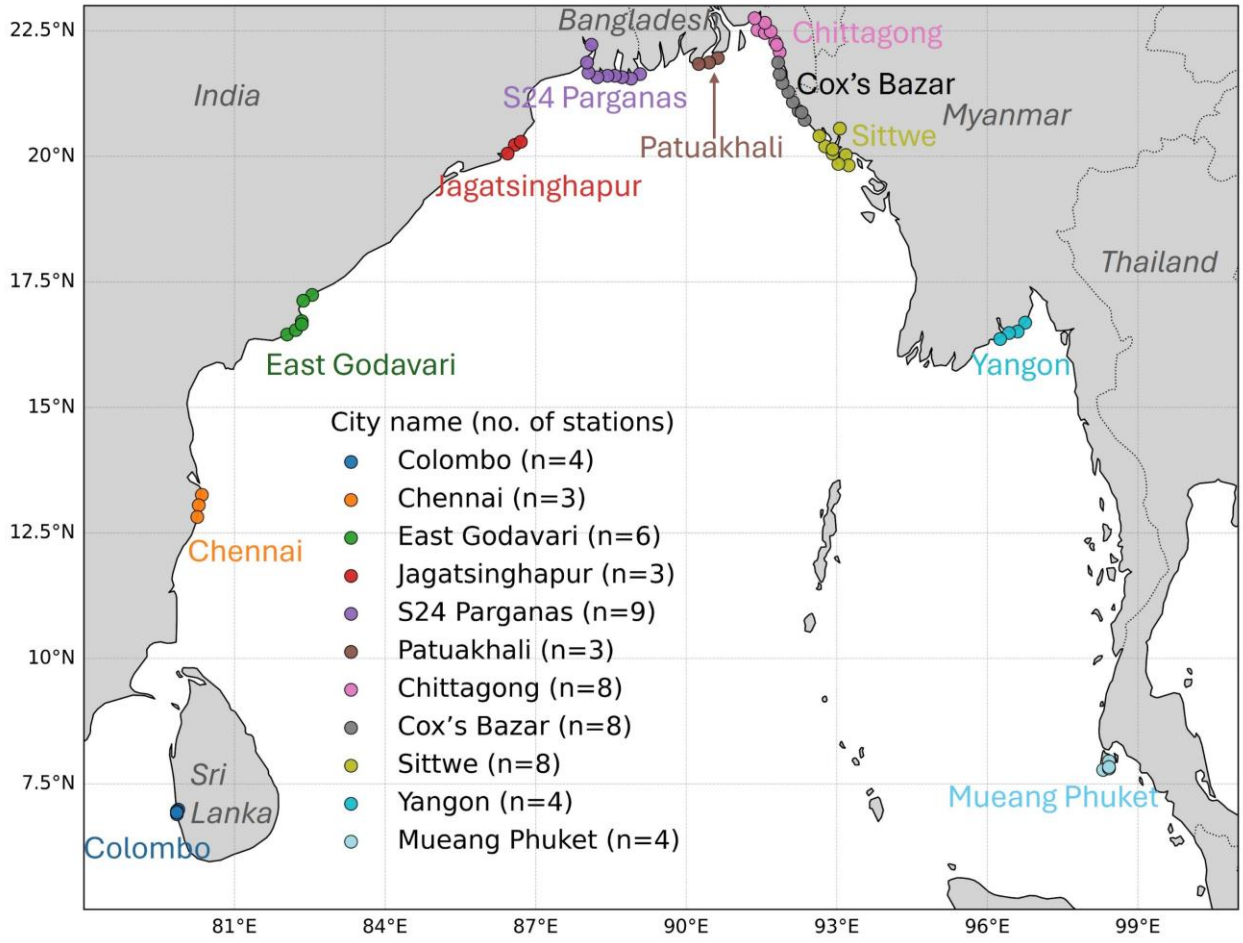

Figure 1. Location of the selected 11 Northeast Indian Ocean cities and virtual stations (point markers) near each target city used for extracting ERA5 surge residual time series and statistical modeling.

Statistical model

In this study, we used extreme value theory (EVT) on annual surge maxima to estimate the probability of extreme surge residuals. The maximum observation for each virtual station is extracted from each fixed-length block (each year) across 1950–2024. The resulting series of maxima are modeled statistically by using four benchmark non-stationary extreme models: Generalized Extreme Value (GEV), Gumbel, Fréchet and EVT-based Bayesian hierarchical Spatially Varying Covariate Model (SVCM) to quantify inter-model uncertainty and tail behavior sensitivity.

Baldan et al., (2022) showed that incorporating non-stationarity through covariate-dependent parameters can improve model fit and alter estimated extremes (e.g., return-level) relative to stationary approaches. Motivated by this, we represent long-term change in annual surge maxima by allowing the location parameter (μ) to vary linearly with time while keeping scale (σ) and shape (ξ) as time-invariant for GEV, Gumbel, and Fréchet formulations. These non-stationary models are fitted independently at each virtual station using Metropolis-Hastings Markov chain Monte Carlo (MCMC) sampler. For each station, we run four parallel chains of 4,000

iterations, discard the first half as burn-in and pool the retained samples to quantify parameter uncertainty and propagate it to return level and trend estimates.

To estimate surge extremes while propagating parameter uncertainty and stabilizing inference across nearby virtual stations within each city, we additionally apply the Bayesian hierarchical Spatially Varying Covariate Model (SVCM; Lu et al., 2025). In SVCM, non-stationarity is introduced by allowing both μ and σ to evolve with time, while ξ is held constant. Because estimating non-stationary parameters independently at each station can be unstable for limited records or weakly informative tails, SVCM uses hierarchical spatial priors so that coefficients vary smoothly over space and information is shared across neighboring stations. Following Lu et al., (2025), we fit SVCM using the No-U-Turn Sampler (NUTS), an adaptive Hamiltonian Monte Carlo algorithm. Similar to other model settings, we run four chains of 4,000 iterations each and adopt a sufficiently high maximum tree depth to ensure adequate explorations of the posterior and good chain mixing.

Non-stationary return period analysis

In a stationary extreme-value model, distribution parameters are constant in time; under nonstationary, one or more parameters vary with a covariate (here, year), so the return level becomes a function of the covariate state. This allows return levels to be evaluated at a chosen baseline year (e.g., 1950 or 2000) rather than interpreting a single curve as representative of the full record-an important advantage for communicating time-varying risk. Following standard practice, the non-exceedance probability associated with an *N*-year return level is

$$P_N = 1 - \frac{1}{N}$$

The *N*-year return level evaluated at a baseline year t_0 is obtained from the quantile function as

$$RL_N(t_0) = \mu(t_0) + \frac{\sigma t_0}{\xi}\left(\left[-\ln\left(1-\frac{1}{N}\right)\right]^{-\xi} - 1\right)$$

To characterize nonstationary changes in hazard without redefining the threshold each year, we fix the baseline surge residual level at $RL_N(t_0)$ (here t_0 = 1950) and then evaluate how frequently that same level would be exceeded under the fitted distribution for another year *t* (e.g., 2000). The exceedance probability in year *t* is

$$P(t) = 1 - F_t(RL_N\,(1950))$$

Where $F_t(.)$ denotes the fitted cumulative distribution function in year *t*. The corresponding effective return period is

$$N_r(t) = \frac{1}{P(t)}$$

Here $N_r(t)$ is interpreted in years under the annual block-maxima assumption. We compute $P(t)$ for each posterior draw and aggregate across draws to obtain credible intervals for $N_r(t)$. By construction, $N_r(1950) = N$ and deviations of $N_r(t)$ from *N* for later years directly quantify changes in the frequency of the same baseline surge level over time. We apply this procedure for

N = {5, 10, 25, 50}. However, we mainly focus on the 50-year return period (and not the 100-year or higher return period) in order to minimize the uncertainty of the extreme value fit.

To account for model selection uncertainty, we construct an ensemble return-period estimate by combining the posterior-based inferences from all four non-stationary statistical formulations (GEV, Gumbel, Fréchet, and SVCM) at each virtual station and city. Specifically, for a given baseline level $RL_N(1950)$ and evaluation year t (e.g., 2000), each model yields a posterior sample of exceedance probability $P_m(t) = 1 - F_{t,\,m}\,(RL_N(1950))$ (and the corresponding $N_{r,\,m}(t) = 1/P_m(t)$), where m indexes the statistical model. We then pool these model-specific posterior draws with equal weight to form an unconditional (model-averaged) ensemble distribution for $P(t)$ and $N_r(t)$ from which we report the multi-model ensemble median as the central estimate and the 25-75% and 5-95% percentiles as uncertainty ranges. This approach preserves within-model parameter uncertainty while explicitly incorporating between-model structural variability in tail assumptions, providing a single robust return-period characterization that is not conditioned on a single distributional choice.

3 Results

3.1 Multi-model ensemble estimates of surge residual return period

Figure 2 compares median of 50-year surge residual return levels (RL50) across four non-stationary statistical models for 11 coastal cities, evaluated at base years 1950 (t1) and 2000 (t2). It highlights both agreement and divergence among the four models. We assess intermodel consistency by showing the spread (defined here as the range) of RL50 at the 1950 baseline and intermodel agreement on the sign of change in RL50 at the 2000 base year relative to 1950. Surge residuals exceeding 1.0 m are mainly found in inner NIO coastal cities (e.g., S24 Parganas, Patuakhali, Chittagong, Cox's Bazar) where the shallow continental shelf amplify tropical cyclone (TC) driven storm surges. As a result, these cities experience higher amplitude but lower probability surge events than cities along the western and eastern NIO cities (T. Islam & Peterson, 2009; M. R. Islam, 2025). In 1950 baseline (t1), the models produce similar RL50 in some cities but markedly different estimates in others. For example, west coasts of NIO (e.g., Colombo, Chennai, East Godavari, and Jagatsinghapur) and Phuket show tightly clustered RL50 distributions – the colored probability density curves (PDF; with surge level on the vertical axis) overlap considerably – indicating high inter-model consistency. In these cases, the difference in the median of RL50 (denoted by the colored dashed horizontal lines) between different statistical models is less than of 0.1 m and corresponding surge residual levels are low (<0.7 m). By contrast, central coasts of NIO (e.g., Patuakhali, Cox's Bazar) where hazard is greatest (>1.6. m) exhibit pronounced inter-model spread: the four PDF curves are relatively more separated and the dashed lines for RL50 span a range of 0.5 m or more. Such divergence is especially evident where Frechet model (purple) projects substantially higher surge residual levels than the Gumbel (orange) or Bayesian (blue) models and in cases the GEV model (green) yields an outlying estimate. For example, Gumbel or Bayesian based framework yields a median of RL50 (~2.2 m) for Chittagong city that corresponds roughly to a median of 1-in-25-year return period event under the Frechet formulation, indicating a substantially higher estimated frequency of occurrence. These disparities underscore non-trivial uncertainty in the RL50 estimates attributable to model choice.

Despite these differences in absolute values, the models are more consistent in the direction of change by 2000 (t2). Figure 2 shows that the implied return period in 2000 (dashed lines) for the fixed 1950 RL50 surge residual varies substantially by city. For instance, in most cities of the west (e.g., Colombo, Chennai, Jagatsinghapur) and east (e.g., Sittwe, Yangon, Phuket) coasts, more than two models agree that a surge residual of the 1950 RL50 magnitude has become less frequent by 2000 (i.e., return period > 50 years). This consensus is visible as each model's 2000 marker lies to the right of 50-year benchmark on the PDF (indicating reduced probability density at that extreme surge level in 2000). In contrast, cities located in the inner NIO (e.g., S24 Parganas, Chittagong, Cox's Bazar) exhibit heightened frequency for the 1950's RL50. For example, if ~2.3 m was a 50-year event in 1950 for Chittagong city, by 2000 at least three models typically suggest it might be a 33-43-year event. Among 11 coastal cities, the sign of change in Patukhali city is strongly model- dependent where two models agree that the 1950 RL50 magnitude has become less frequent by 2000, however, remaining two models disagreed with it. It is also noticeable that Sittwe shows a bimodal distribution of surge residual (Fig. 2). This pattern is mainly driven by one virtual station behaves differently from the others. Its annual maximum surge levels are consistently much lower than those at the remaining stations. This station is located farther inland (Supplementary Fig. 1), which may reduce its exposure to surge influence. In summary, the intermodel differences shown in the Fig. 2 reinforce the need to use an ensemble of statistical models to evaluate return levels and their changes, rather than over-confidence on single model's output.

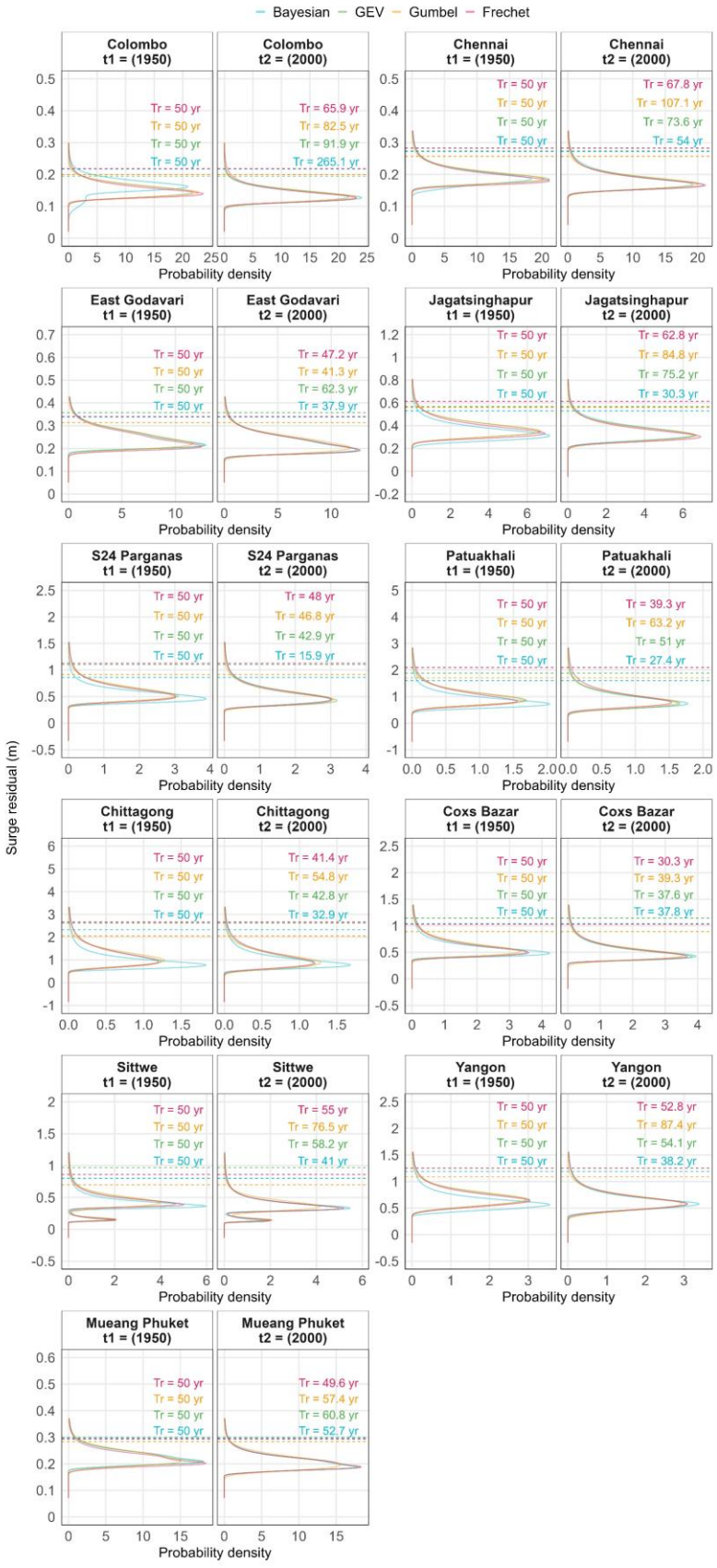
Bayesian GEV Gumbel Frechet
Colombo t1 = (1950)
Tr = 50 yr
Tr = 50 yr
Tr = 50 yr
Tr = 50 yr
Colombo t2 = (2000)
Tr = 65.9 yr
Tr = 82.5 yr
Tr = 91.9 yr
Tr = 265.1 yr
Chennai t1 = (1950)
Tr = 50 yr
Tr = 50 yr
Tr = 50 yr
Tr = 50 yr
Chennai t2 = (2000)
Tr = 67.8 yr
Tr = 107.1 yr
Tr = 73.6 yr
Tr = 54 yr
East Godavari t1 = (1950)
Tr = 50 yr
Tr = 50 yr
Tr = 50 yr
Tr = 50 yr
East Godavari t2 = (2000)
Tr = 47.2 yr
Tr = 41.3 yr
Tr = 62.3 yr
Tr = 37.9 yr
Jagatsinghapur t1 = (1950)
Tr = 50 yr
Tr = 50 yr
Tr = 50 yr
Tr = 50 yr
Jagatsinghapur t2 = (2000)
Tr = 62.8 yr
Tr = 84.8 yr
Tr = 75.2 yr
Tr = 30.3 yr
S24 Parganas t1 = (1950)
Tr = 50 yr
Tr = 50 yr
Tr = 50 yr
Tr = 50 yr
S24 Parganas t2 = (2000)
Tr = 48 yr
Tr = 46.8 yr
Tr = 42.9 yr
Tr = 15.9 yr
Patuakhali t1 = (1950)
Tr = 50 yr
Tr = 50 yr
Tr = 50 yr
Tr = 50 yr
Patuakhali t2 = (2000)
Tr = 39.3 yr
Tr = 63.2 yr
Tr = 51 yr
Tr = 27.4 yr
Chittagong t1 = (1950)
Tr = 50 yr
Tr = 50 yr
Tr = 50 yr
Tr = 50 yr
Chittagong t2 = (2000)
Tr = 41.4 yr
Tr = 54.8 yr
Tr = 42.8 yr
Tr = 32.9 yr
Coxs Bazar t1 = (1950)
Tr = 50 yr
Tr = 50 yr
Tr = 50 yr
Tr = 50 yr
Coxs Bazar t2 = (2000)
Tr = 30.3 yr
Tr = 39.3 yr
Tr = 37.6 yr
Tr = 37.8 yr
Sittwe t1 = (1950)
Tr = 50 yr
Tr = 50 yr
Tr = 50 yr
Tr = 50 yr
Sittwe t2 = (2000)
Tr = 55 yr
Tr = 76.5 yr
Tr = 58.2 yr
Tr = 41 yr
Yangon t1 = (1950)
Tr = 50 yr
Tr = 50 yr
Tr = 50 yr
Tr = 50 yr
Yangon t2 = (2000)
Tr = 52.8 yr
Tr = 87.4 yr
Tr = 54.1 yr
Tr = 38.2 yr
Mueang Phuket t1 = (1950)
Tr = 50 yr
Tr = 50 yr
Tr = 50 yr
Tr = 50 yr
Mueang Phuket t2 = (2000)
Tr = 49.6 yr
Tr = 57.4 yr
Tr = 60.8 yr
Tr = 52.7 yr
Surge residual (m)
Probability density

Figure 2. Intermodel comparison of nonstationary 50-year surge residual return levels (RL50) and implied frequency change. For each of 11 NIO cities, panels show model specific probability density functions (PDFs; colored curves) of RL50 estimated from annual surge residual maxima over 1950-2024 using four nonstationary statistical formulations (Bayesian, GEV, Gumbel, Frechet). The left panel for each city (t1=1950) summarizes the posterior distribution of RL50 at the 1950 baseline year. In the right panel for each city (t2=2000), the colored PDFs are derived from the year-2000 fitted nonstationary distribution but they summarize the distribution of the implied return period in 2000 for the fixed RL50 defined in 1950. Dashed horizontal lines denote posterior medians (RL50 in t1; implied return period in t2).

The ensemble summary in Fig. 3 condensed the four-model spread shown in Fig. 2 into a single probabilistic description of the RL50 for each city. While Fig. 2 revealed very tight clustering across models for Colombo, Chennai, East Godavari, Jagatsinghapur, and Phuket, the ensemble bands here correspondingly narrow. It confirmed that structural uncertainty in RL50 is small (e.g., the 25-75% range is only a few centimeters wide). In contrast, cities that showed relatively large intermodel spread in Fig. 2 (S24 Parganas, Patukhali, Chittagong, Cox's Bazar) display broad ensemble bands (Fig. 3), with 25-75% intervals spanning several decimeters to a meter. This quantified substantial uncertainty in the underlying extreme surge residual level that was apparent in Fig. 2 qualitatively.

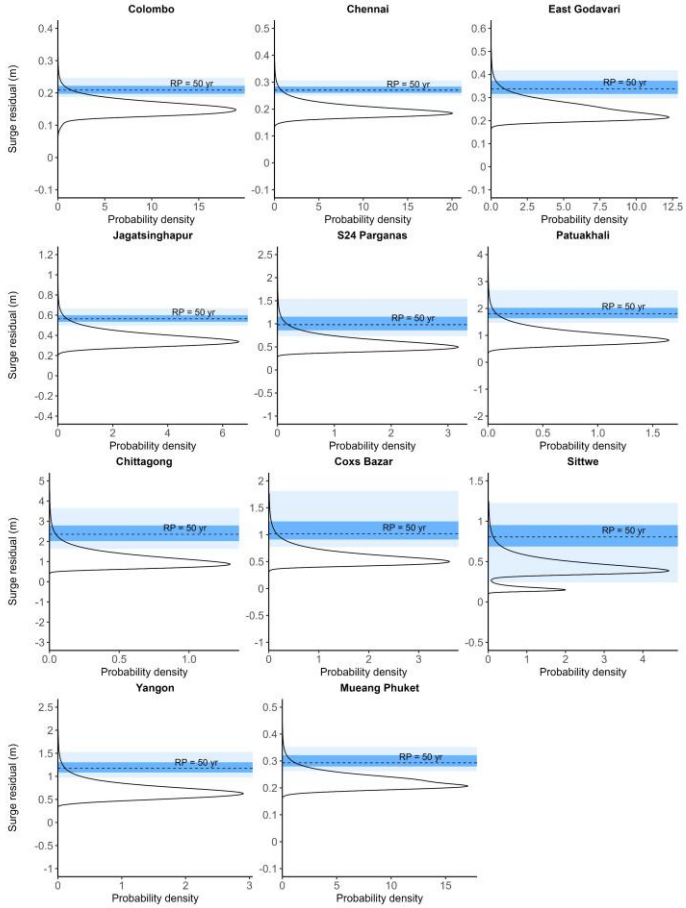

Figure 3. Ensemble estimate of nonstationary RL50 at the 1950 baseline year. For each of 11 NIO cities panels show the ensemble PDF (black colored curve) of RL50 derived by combining posterior samples from the four nonstationary statistical formulations (Bayesian, GEV, Gumbel, Frechet) fitted to annual surge residual maxima over 1950-2024. The dotted horizontal line denotes the ensemble median RL50 for 1950, while shaded bands indicate ensemble uncertainty ranges (dark shading: 25^{th}-75^{th} percentiles; light shading: 5^{th}-95^{th} percentiles).

Fig. 4 further reveals the temporal change in RL50. Along the western and outer eastern margins of the NIO (e.g., Colombo, Chennai, Jagatsinghapur, Phuket), the 1950 RL50 becomes rarer by 2000. It implies that return periods increase from 50-years to about 55-104 years (or median annual exceedance probability reduced by 9%-52%). At several other cities (e.g., East Godavari, Sittwe, Yangon), the ensemble return period remains close to 50-years in 2000, indicating little net change. In contrast, inner NIO cities around the head of the Bay (S24 Parganas, Patuakhali, Chittagong, Cox's Bazar) show the opposite behavior: the 1950 RL50 becomes more frequent in the ensembles, with return periods shortened to roughly 33-39 years. This corresponds to an increase in median annual exceedance probability up to 51%, making the same 1950-design RL50 measurably more likely by 2000. However, these cities, particularly Patuakhali, where the individual models in Fig. 2 disagreed on the sign of change also exhibit visibly wide uncertainty bands. It suggests that the inferred changes there are less robust than at other cities.

In addition to RL50, we also assessed change in the 5-, 10-, and 25-year return periods (here after RL5, RL10, and RL25) at the 2000 base year relative to 1950 (Fig. 4). Although the magnitude of change depends on the specified return periods, the spatial distribution of changes is largely consistent with the RL50 results. The hazard levels in Colombo, Chennai, Jagatsinghapur, and Phuket increase while there are comparatively small net changes at East Godavari, Sittwe, Yangon. Along the western and outer eastern NIO coasts, return periods in 2000 tend to be longer than in 1950 across all three thresholds, indicating a systematic reduction (median annual exceedance probability decreased by 15%-58%) in the frequency of those surge events. In contrast, inner NIO cities around the head of the Bay (S24 Parganas, Patuakhali, Chittagong, Cox's Bazar) exhibit a more scale-dependent behavior. The implied return periods in 2000 remain close to their nominal values for lower return period thresholds (e.g., RL5, RL10; Fig. 4), whereas, it shorten markedly for rarer events (e.g., RL25), in line with the RL50 results in Fig. 4. This corresponds to an increase in median annual exceedance probability up to 31% for 1 in 25-year surge events by 2000.

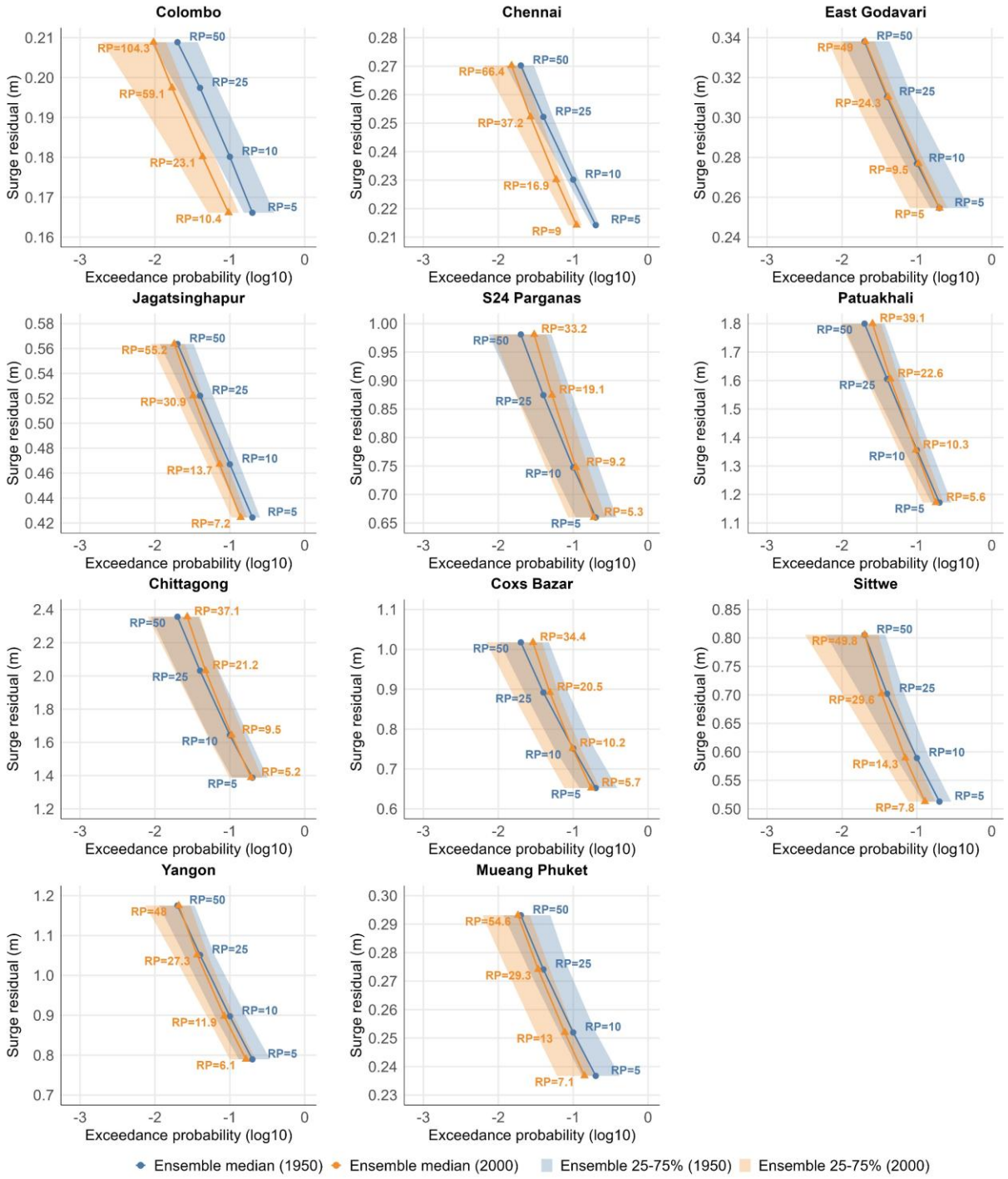

Figure 4. Ensemble exceedance curves for fixed baseline return levels and implied return-period shifts between 1950 and 2000. For each of 11 NIO cities, panels show ensemble median exceedance probability (log10 scale) as a function of surge residual level for two baseline years: 1950 (blue) and 2000 (orange). Points along each curve correspond to the 1950 baseline return levels for N = 5, 10, 25, and 50 years (labels "RP = 5, 10, 25, 50"), plotted as their exceedance probabilities under the fitted distributions at 1950 and 2000. The orange annotations report the implied return periods in 2000 for the same fixed surge thresholds defined by the 1950 return

levels. Shaded bands indicate ensemble uncertainty (25^{th}-75^{th} percentile range) for 1950 (blue) and 2000 (orange).

To further evaluate whether the scale-dependent behavior in Fig. 4 is reproducible under climate-model forcing, we repeated the same return level estimation (RL5, RL10, RL25, and RL50) using HighResMIP-driven historical surge residual time series (Fig. 5). Throughout, we treat ERA5 as a reference baseline and interpret this as a historical benchmarking exercise, not a formal climate model validation of future projections. The HighResMIP surge residual archive includes outputs forced by five climate models (CMCC-CM2-VHR4, EC-Earth3P-HR, GFDL-CM4C192-SST, HadGEM3-GC31-HM, and HadGEM3-GC31-HM-SST). However, only EC-Earth3P-HR provides a continuous historical timeseries beginning in 1950, with availability through 2014 (Copernicus Climate Change Service, 2025). Accordingly, we restrict this comparison to EC-Earth3P-HR (1950-2014), re-compute the ERA5-driven return levels over the same 1950-2014 period, and then evaluate city-wise agreement between the climate model-forced and the ERA5-forced estimates. Across the 11 coastal cities, the median return levels for RL5, RL10, RL25, and RL50 at the 1950 base year show strong spatial correspondence between HighResMIP and ERA5 (Pearson $r > 0.9$). Importantly, for the inner NIO cities (S24 Parganas, Patuakhali, Chittagong, Cox's Bazar), HighResMIP reproduces the ERA5-inferred sign of change both for the lower (RL5 and RL10) and higher (RL25 and RL50) thresholds at the 2000 base year relative to 1950 (Fig. 5). In contrast, agreement for other cities is weaker and in several cases mixed across forcings. This comparison should be interpreted as a limited historical benchmark rather than a comprehensive validation of future projections. Because it uses only a single HighResMIP model (EC-Earth3P-HR) and therefore does not sample the full spread of climate-model forcing uncertainty. Nevertheless, the consistent sign of change for RL25-RL50 in the inner NIO suggests that the most extreme surge residual levels defined at the 1950 baseline tend to occur more frequently by 2000 than moderate events. This highlights the increased risk from the largest events along the densely populated coasts of West Bengal (India) and Bangladesh.

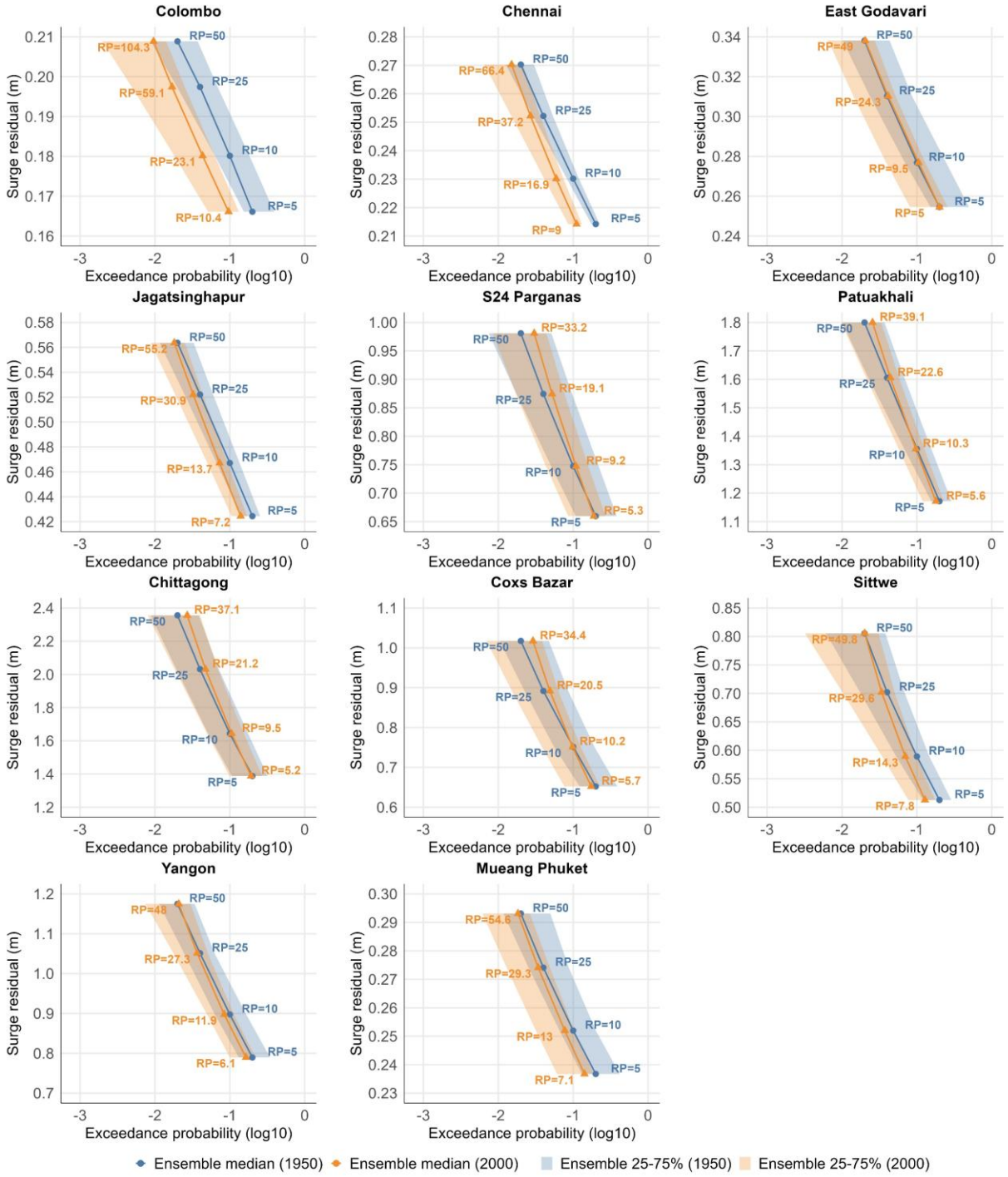

Figure 5. Same as Fig. 4 but using HighResMIP (ensemble member: EC-Earth3P-HR)-driven historical surge residual time series.

3.2 Multi-model ensemble estimates of long term surge residual trend

Figure 6 complements the return-level diagnostics (Figs. 2-4) by examining whether the same reanalysis record exhibits coherent long-term changes in annual maximum surge residual (1950-2024), and by separating structural spread across four non-stationary models from an

ensemble summary. It generally yields negative trend estimates (~ - 1 mm/year) across the 11 coastal cities, indicating an overall weakening of surge residual annual maxima in the ERA5-driven estimates. Spatial distribution of this change is provided in the supplementary materials (Fig. S3). Consistent with the intermodel behavior seen for return levels (Fig. 2), Fig. 6a shows model agreement is strongest at several western and southern margin (e.g., Colombo, Chennai, East Godavari, Phuket) where trend magnitudes (- < 1 mm/year) are similar and uncertainty intervals are comparatively narrow. In contrast, the largest spread occurs in the greater hazard-prone areas (S24 Parganas, Patuakhali, Chittagong, Cox's Bazar). Among all, the Bayesian specification often widens uncertainty and, in some cases, brings intervals close to or beyond zero (towards positive)-demonstrating uncertainty not only in magnitudes but also in whether the decline is distinguishable from no change. Sittwe and Yangon fall between these extremes: point estimates remain negative, but uncertainty is larger than at the western sites. The multi-model ensemble median synthesis in Fig. 6b remains negative but most precisely constrained where models agree and least constrained where Fig. 6a shows pronounced intermodel divergence. This generally negative surge residual trend is also broadly consistent with the return-period results for several cities where 1950 return levels become less frequent (or shows little net change; Figs. 2-4) by 2000. However, Fig. 6 does not fully explain the cases where rarer thresholds (e.g., RL25, RL50) become more frequent by 2000 at inner NIO cities (Fig. 4). This is not unexpected because return period shifts for rare events depend more on tail behavior and model structure than on the linear trend in annual maxima alone.

Importantly, Fig. 6b also places changes in the broader extreme sea level context by showing that CMIP6 based mean sea level (MSL) trends are uniformly positive (~ 1 mm/year). It tightly constrained across all cities and opposite in sign to the surge residual-maxima trends. The negative surge residual-maxima trends and positive MSL trends are of similar order (mm/year), suggests that their net effect on total ESL could partially offset. Nevertheless, we do not treat this as robust constraint because our MSL estimates are derived from the climate model (CMIP6), whereas observational studies (tide gauges/altimetry) have reported larger rise rates in some regions of NIO (Dewan et al., 2025; Carvalho & Wang, 2019; Tariq Masood Ali Khan, 2000). Integrating those sources is non-trivial here because they are not co-located with the hydrodynamic model output points used for the surge residual and MSL series and would require additional spatial/vertical harmonization which is beyond the scope of this study.

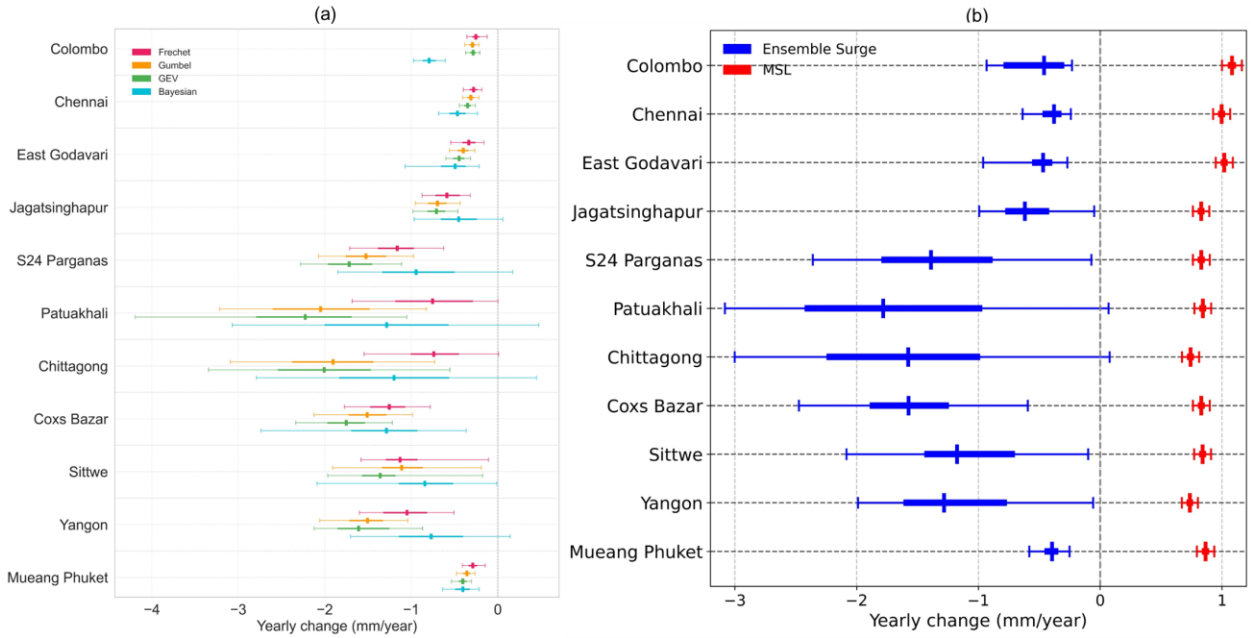

Figure 6. Surge residual annual-maximum trends across 11 NIO cities. (a) city wise inter-model estimates of trends during 1950-2024 from the four nonstationary statistical formulations (Bayesian, GEV, Gumbel, Frechet); (b) ensemble surge residual trend uncertainty (blue) compared with MSL trend uncertainty (red). MSL trends were estimated using ordinary linear regression. Points indicate posterior medians and horizontal whiskers show uncertainty intervals.

3.3 Differences in surge residual bias reporting for HighResMIP ensemble

Figure 7 quantifies how the reported bias of HighResMIP against ERA5 reanalysis at the RL50 depends on the statistical model used to translate time series into return levels. Across most cities, median biases are predominantly negative for GEV, Gumbel, Bayesian, and statistical ensemble, implying that HighResMIP tends to produce lower RL50 than the ERA5 reference baselines. The magnitude of this underestimation is modest at several cities which exhibit lower surge risks. At Colombo, Chennai, East Godavari, Phuket, typical median biases is in the order of ~-0.1 m (GEV/Gumbel/Bayesian), and their multi-model ensemble medians are approximately -0.05 m. However, the sensitivity to model choice becomes most evident where hazards are greatest. For instance, at Chittagong, the median bias ranges from ~0.1 m (Frechet) to ~-0.6 m (Gumbel), ~-0.9 m (GEV) and ~-1.8 m (Bayesian), with the multi-model ensemble median ~-0.7 m. Likewise, for Cox's Bazar and Yangon, median underestimation spans roughly ~0 m to ~-0.5 m. These differences demonstrate that the quantification of the bias in HighResMIP at RL50 is substantially affected by the choice of the statistical model to estimate tail behavior. We further confirmed similar tendencies for RL5, RL10, and RL25 estimates (Supplementary Figs. S4-6).

A consistent feature across panels in Fig. 7 is that the Frechet-based bias median is closest to zero for the 11 coastal cities, suggesting that Frechet yields the most favorable median bias summary. Nevertheless, the same figure shows why median values cannot fully explain the accuracy of models. In several high hazard cities (e.g., Patuakhali, Chittagong, Cox's Bazar), the Frechet credible bands remain wide, indicating that a near zero median can co-exist with substantial posterior uncertainty in the inferred bias. Moreover, sign reversals occur in some

cities. For example, at Jagatsinghapur, Frechet and Bayesian medians are positive (0.02 m to 0.07 m) while GEV and Gumbel are negative (-0.11 m to -0.13 m), meaning the direction of bias itself can be model dependent. In this context, the statistical ensemble bias provides a more transparent summary where the median typically lies between the single model estimates. Also, its credible interval reflects the uncertainty that would be hidden by selecting one preferred statistical distribution. In summary, Fig. 7 suggests that reanalysis-based (e.g., ERA5) bias reporting for climate models (e.g., HighResMIP) at design relevant return levels is not invariant to statistical model choice. The ensemble approach of statistical models is therefore safer basis for evaluation. Because it can reduce dependence on any single tail assumption and avoid over-confident narratives based on one distribution that may not be universally appropriate across places.

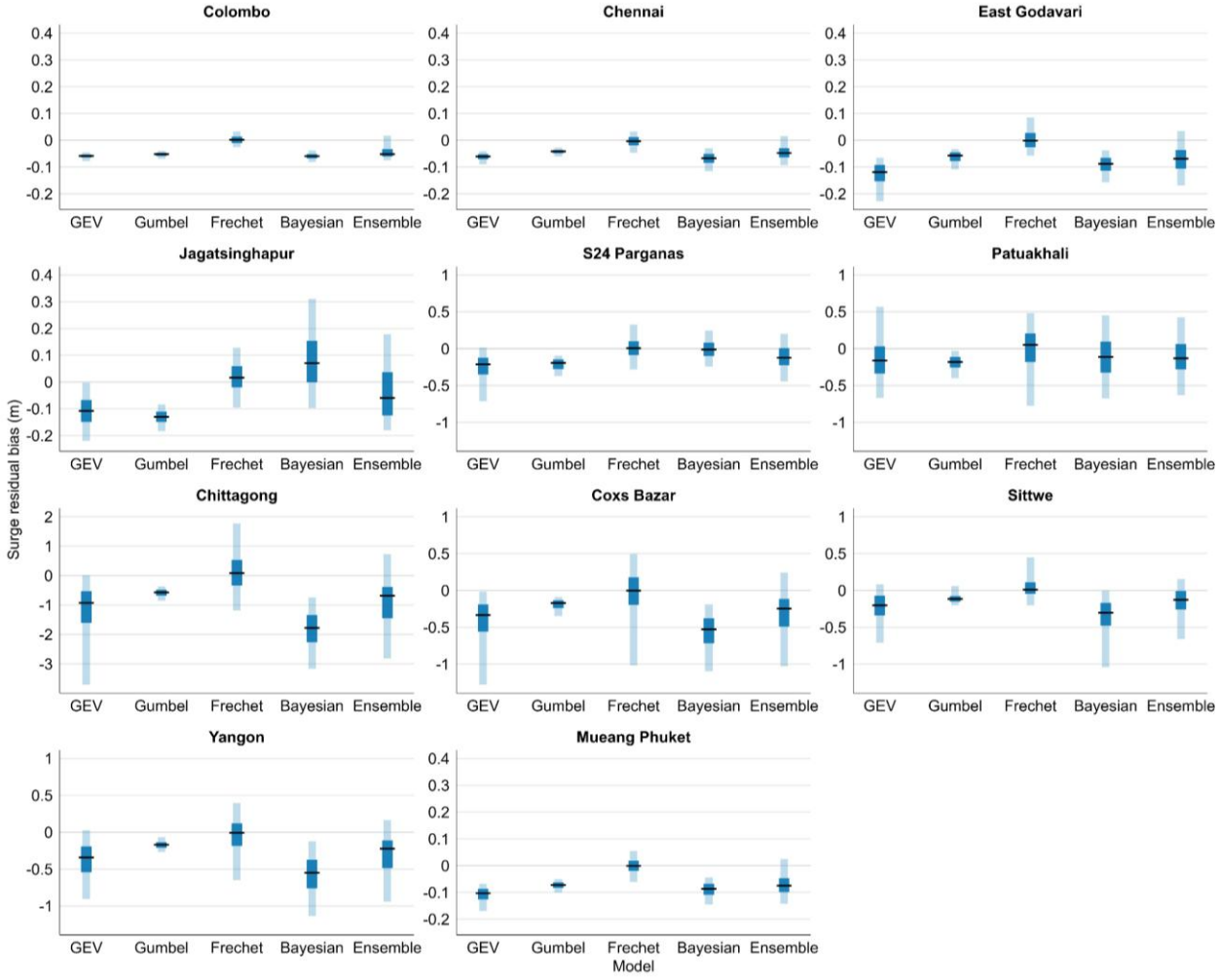

Figure 7. City-wise distribution of RL50 bias (HighResMIP minus ERA5 estimate) for five statistical approaches (Bayesian, GEV, Gumbel, Frechet, and multi-model ensemble). Dark shading indicates the 25th-75th percentile range and light shading the 5th-95th percentile range.

4 Conclusions and Discussion

Reanalysis-based storm surge products offer a practical foundation for estimating coastal extremes in data-sparse regions, yet the common practice of adopting a single extreme value model leaves model selection uncertainty largely invisible in design-relevant metrics. Here we use the Copernicus ERA5-driven surge residual record (1950-2024) to evaluate extremes for 11 Northeast Indian Ocean (NIO) cities through a non-stationary, multi-model statistical framework that integrates classical EVT families and Bayesian formulations. To our knowledge, this is the first study to assess return levels, implied return-period shifts, and long-term surge trends in data sparse NIO cities while explicitly quantifying model choice uncertainty. The results reveal strong spatial heterogeneity. In central (inner) NIO cities (S24 Parganas, Patuakhali, Chittagong, Cox's Bazar), multi-models agree that the 1950-defined rare events (e.g., RL25, RL50) become noticeably more frequent by 2000, even though annual maximum surge residual trends over 1950-2024 are negative (~ -1 mm/y). In contrast, several western and outer western margins of NIO cities (e.g., Colombo, Chennai) show the opposite tendency with longer implied return periods. Inter-model contrasts are largest where surge hazard is greatest (e.g., central NIO cities) and model choice can greatly change inferred design levels. For example, Gumbel/Bayesian estimates of RL50 medians are aligned with roughly RL25 under Frechet estimates, underscoring the need for ensemble statistical reporting. Finally, when benchmarking HighResMIP-driven surge residual extremes against the ERA5 reference, the magnitude and even interpretation of return level bias reporting depends on the statistical model used. It suggests an ensemble of statistical models provides a more conservative and transparent basis for skill assessment than single-model summaries.

The spatial and scale-dependent changes suggest that the evolution of surge hazard across the NIO is unlikely to be spatially uniform or controlled by a single mechanism. The inner NIO cities are surge sensitive because coastal geometry and shallow shelves promote large surge amplification and strong tide-surge interactions. Therefore, relatively small changes in storm approach, landfall location, or storm structure can produce large changes in the extreme surge levels compared with open-coast settings (e.g., western NIO cities). Observational analyses of northern Bay of Bengal TC landfalls indicate that an eastward shift in the median strike location toward westernmost Bangladesh after 1960, with strong spatial differences in TC impacts across zones that include the West Bengal (India) and Bangladesh coasts (Bandyopadhyay et al., 2021). Such a redistribution of landfall exposure likely generated the kind of uneven spatial pattern seen in our implied return-period changes. Importantly, the fact that changes are strongest for rarer thresholds (RL25-RL50) is also physically consistent with changes concentrated in the greater surge residual-generating events. Balaguru et al. (2014) show that the intensity of post-monsoon (October-November) major TCs (maximum sustained wind speed > 49 m/s) in Bay of Bengal increased during 1981-2010, a shift that likely affected the upper tail. In contrast, moderate events (RL5-RL10) remain less affected likely because they are generally influenced by a broader mix of storm types (monsoon depressions, weaker TCs, synoptic storms). This framing also helps reconcile why RL25-RL50 can become frequent by 2000 in inner cities (Fig. 4), although linear trend in annual surge residual maxima over 1950-2024 is negative (Fig. 6). Single long-term trend summarizes changes in typical annual maxima across the full record, while implied return period changes for fixed rare thresholds are governed by the tail behavior and event composition, which

can be evolved nonlinearly over time. Nevertheless, robust attribution will require event-based diagnostics that link annual maxima to storm characteristics and separate TC and non-TC contributions.

Uncertainty-informed estimation of design-relevant return levels/periods is particularly important in data-sparse coastal regions. Because the short or missing tide-gauge records often preclude robust analysis of local extremes and motivate reliance on reanalysis-driven or model-based surge products (Tadesse & Wahl, 2021). In practice, engineers and risk practitioners commonly use return levels/periods to define flood zones and inform infrastructure design. Therefore, under-reporting uncertainty can translate directly into maladaptation or overconfidence in protection standards (Wahl et al., 2017). Our results reinforce this concern by showing that, even with a fixed physical dataset, the statistical translation layer can significantly change inferred design levels and implied frequencies-an issue that broad-scale coastal assessments have historically tended to overlook. More generally, previous work has demonstrated that uncertainties in present day ESL estimates can be comparable to or exceed other major uncertainty sources (e.g., sea level rise projection) relevant for planning. This differences among-extreme value methods can propagate into inundation and adaptation decisions (Wahl et al., 2017). In this context, explicitly considering statistical model selection uncertainty provides a more defensible basis for design. Also, statistical model selection uncertainty is useful to benchmark climate model-surge extremes against reanalysis in regions where observational constraints remain limited (Muis et al., 2016).

There are several limitations that should be considered when interpreting the results shown in this study. First, we acknowledge that ERA5-driven surge residual product is not intended for detailed local-scale surge assessment in complex estuaries or semi-enclosed bays (Aleksandrova et al., 2025; Copernicus Climate Change Service, 2025). Therefore, our city-scale virtual station approach cannot fully resolve local nearshore processes. This limitation may bias the characterization of local extreme surges. Nevertheless, our objective is not estimating site-specific engineering design thresholds. Rather it is to evaluate how statistical model choice affects the estimation of surge extremes across a consistent set of data-sparse coastal cities. For this purpose, ERA5-driven surge residual product provides a uniquely suitable and regionally consistent baseline. Accordingly, our results should be interpreted as comparative assessment of uncertainty-aware extreme surge metrics at city-scale. Second, while we quantify statistical model selection uncertainty using an ensemble of nonstationary formulations, parameter uncertainty inherent to each statistical model remained unquantified and our nonstationary is represented with relatively simple time dependance (e.g., linear evolution of parameters). Therefore, addressing parameter uncertainty, introducing alternative co-variates (e.g., storm track metrics, large scale climate indices), and considering non-linear changes of parameters could yield different tail behavior and trend attribution. Third, we observe that intermodel spread tends to be larger in cities with higher surge hazard and smaller where surges are modest. The processes driving this relationship remain unclear and should be examined in future work. Fourth, the HighResMIP validation is necessarily constrained by data availability: only a subset of the HighResMIP-driven surge record is continuous back to 1950, limiting the extent to which multi-model climate-forced spread can be fully contrasted with reanalysis across the entire 1950-2024 period. Finally, our analyses focus on surge residuals and annual maxima; isolating the

mechanisms behind the inner-basin increase in rare event frequency would require event-based diagnostics that separate TC and non-TC contributions and examine changes in tail shape, storm approach, and seasonality. Future work should therefore (i) extend the uncertainty framework to include model-specific parameter uncertainty, multiple reanalysis, and alternative surge residual reconstructions, (ii) incorporate more flexible nonstationary structures and physically interpretable covariates, (iii) reconcile and co-locate independent MSL products with model nodes for integrated ESL assessment, and (iv) develop event-based attribution analyses linking surge extremes to storm characteristics. Together, these steps would strengthen confidence in design-relevant return levels and improve the interpretability of historical changes in coastal surge hazard across the NIO.

Acknowledgment

The authors declare no financial or conflict of interest. This work is supported by JST Moonshot R&D project (grant no. JPMJMS2281). We acknowledge the support by JSPS Grant-in-Aid for Early-Career Scientists (Grant No. 23K13531) and the Obayashi Foundation research grant.

Open Research

ERA5 and HighResMIP storm surge time series and MSL data can be downloaded from Copernicus Climate Change Service (2025).

References

Alamgir, M., Hashim, M., Pour, A. B., & Shahid, S. (2025). Transformation in the sea surface properties of the Bay of Bengal under climate change. *Ocean Dynamics*, *75*(9), 76. https://doi.org/10.1007/s10236-025-01715-1

Aleksandrova, N., Veenstra, J., & Muis, S. (2025, September 3). Global dataset of storm surges and extreme sea levels for 1950–2024 based on the ERA5 climate reanalysis. Copernicus GmbH. https://doi.org/10.5194/essd-2025-471

Balaguru, K., Taraphdar, S., Leung, L. R., & Foltz, G. R. (2014). Increase in the intensity of postmonsoon Bay of Bengal tropical cyclones. *Geophysical Research Letters*, *41*(10), 3594–3601. https://doi.org/10.1002/2014GL060197

Baldan, D., Coraci, E., Crosato, F., Ferla, M., Bonometto, A., & Morucci, S. (2022). Importance of non-stationary analysis for assessing extreme sea levels under sea level rise. *Natural Hazards and Earth System Sciences*, *22*(11), 3663–3677. https://doi.org/10.5194/nhess-22-3663-2022

Bandyopadhyay, S., Dasgupta, S., Khan, Z. H., & Wheeler, D. (2021). Spatiotemporal Analysis of Tropical Cyclone Landfalls in Northern Bay of Bengal, India and Bangladesh. *Asia-Pacific Journal of Atmospheric Sciences*, *57*(4), 799–815. https://doi.org/10.1007/s13143-021-00227-4

Beck, N., Genest, C., Jalbert, J., & Mailhot, M. (2020). Predicting extreme surges from sparse data using a copula-based hierarchical Bayesian spatial model. *Environmetrics*, *31*(5), e2616. https://doi.org/10.1002/env.2616

Becker, M., Seeger, K., Paszkowski, A., Marcos, M., Papa, F., Almar, R., et al. (2024). Coastal Flooding in Asian Megadeltas: Recent Advances, Persistent Challenges, and Call for Actions Amidst Local and Global Changes. *Reviews of Geophysics*, *62*(4), e2024RG000846. https://doi.org/10.1029/2024RG000846

Boettle, M., Rybski, D., & Kropp, J. P. (2016). Quantifying the effect of sea level rise and flood defence – a point process perspective on coastal flood damage. *Natural Hazards and Earth System Sciences*, *16*(2), 559–576. https://doi.org/10.5194/nhess-16-559-2016
Cael, B. B., Burger, F. A., Henson, S. A., Britten, G. L., & Frölicher, T. L. (2024). Historical and future maximum sea surface temperatures. *Science Advances*, *10*(4), eadj5569. https://doi.org/10.1126/sciadv.adj5569
Caruso, M. F., & Marani, M. (2022). Extreme-coastal-water-level estimation and projection: a comparison of statistical methods. *Natural Hazards and Earth System Sciences*, *22*(3), 1109–1128. https://doi.org/10.5194/nhess-22-1109-2022
Carvalho, K. S., & Wang, S. (2019). Characterizing the Indian Ocean sea level changes and potential coastal flooding impacts under global warming. *Journal of Hydrology*, *569*, 373–386. https://doi.org/10.1016/j.jhydrol.2018.11.072
Chen, Z., Zhou, T., Zhang, L., Chen, X., Zhang, W., & Jiang, J. (2020). Global Land Monsoon Precipitation Changes in CMIP6 Projections. *Geophysical Research Letters*, *47*(14), e2019GL086902. https://doi.org/10.1029/2019GL086902
Coles, S. (2001). *An Introduction to Statistical Modeling of Extreme Values*. London: Springer. https://doi.org/10.1007/978-1-4471-3675-0
Copernicus Climate Change Service. (2025). Global sea level change time series from 1950 to 2050 derived from reanalysis and high resolution CMIP6 climate projections [Data set]. Retrieved from https://cds.climate.copernicus.eu/datasets/sis-water-level-change-timeseries-cmip6?tab=overview
Dewan, A., Jain, H., Hossain, M. A., Adnan, M. S. G., & Mahmud, M. R. (2025). Estimating vertical land motion-adjusted sea level rise in a data-sparse and vulnerable coastal region. *Geomatics, Natural Hazards and Risk*, *16*(1), 2545375. https://doi.org/10.1080/19475705.2025.2545375
Dullaart, J. C. M., Muis, S., Bloemendaal, N., & Aerts, J. C. J. H. (2020). Advancing global storm surge modelling using the new ERA5 climate reanalysis. *Climate Dynamics*, *54*(1), 1007–1021. https://doi.org/10.1007/s00382-019-05044-0
Enríquez, A. R., Wahl, T., Marcos, M., & Haigh, I. D. (2020). Spatial Footprints of Storm Surges Along the Global Coastlines. *Journal of Geophysical Research: Oceans*, *125*(9), e2020JC016367. https://doi.org/10.1029/2020JC016367
Flowerdew, J., Mylne, K., Jones, C., & Titley, H. (2013). Extending the forecast range of the UK storm surge ensemble. *Quarterly Journal of the Royal Meteorological Society*, *139*(670), 184–197. https://doi.org/10.1002/qj.1950
Hersbach, H., Bell, B., Berrisford, P., Hirahara, S., Horányi, A., Muñoz-Sabater, J., et al. (2020). The ERA5 global reanalysis. *Quarterly Journal of the Royal Meteorological Society*, *146*(730), 1999–2049. https://doi.org/10.1002/qj.3803
Hoshino, S., Esteban, M., Mikami, T., Takagi, H., & Shibayama, T. (2016). Estimation of increase in storm surge damage due to climate change and sea level rise in the Greater Tokyo area. *Natural Hazards*, *80*(1), 539–565. https://doi.org/10.1007/s11069-015-1983-4
Islam, M. R. (2025). Tropical cyclones in Bangladesh: retrospective analysis of storm information, disaster statistics, and preparedness. *Environmental Research Communications*, *7*(1), 015003. https://doi.org/10.1088/2515-7620/ada239

Islam, M. R., Satoh, M., & Takagi, H. (2022). Tropical Cyclones Affecting Japan Central Coast and Changing Storm Surge Hazard since 1980. *Journal of the Meteorological Society of Japan. Ser. II*, *100*(3), 493–507. https://doi.org/10.2151/jmsj.2022-024
Islam, M. R., Duc, L., & Sawada, Y. (2023). Assessing Storm Surge Multiscenarios Based on Ensemble Tropical Cyclone Forecasting. *Journal of Geophysical Research: Atmospheres*, *128*(23), e2023JD038903. https://doi.org/10.1029/2023JD038903
Islam, M. R., Duc, L., Sawada, Y., & Satoh, M. (2023). Does mean sea level trend mask historical storm surge trend: evidence from tropical cyclones affecting Japan since 1980. *Environmental Research Letters*, *18*(8), 085004. https://doi.org/10.1088/1748-9326/ace985
Islam, M. R., Oizumi, T., Duc, L., Ota, T., Kawabata, T., & Sawada, Y. (2026). Beyond the Single Hazard Framework: A Proof of Concept Study of Multi-Hazard Worst Case Scenarios from Ensemble Forecasts of Tropical Cyclone Hagibis (2019). https://doi.org/10.1175/WAF-D-25-0030.1
Islam, T., & Peterson, R. E. (2009). Climatology of landfalling tropical cyclones in Bangladesh 1877–2003. *Natural Hazards*, *48*(1), 115–135. https://doi.org/10.1007/s11069-008-9252-4
Kato, F., & Tajima, Y. (2023). Coastal adaptation to climate change in Japan: a review. *Coastal Engineering Journal*, *65*(4), 597–619. https://doi.org/10.1080/21664250.2023.2259187
Kosaka, Y., Kobayashi, S., Harada, Y., Kobayashi, C., Naoe, H., Yoshimoto, K., et al. (2024). The JRA-3Q Reanalysis. *Journal of the Meteorological Society of Japan. Ser. II*, *102*(1), 49–109. https://doi.org/10.2151/jmsj.2024-004
Li, H., Haer, T., Couasnon, A., Enríquez, A. R., Muis, S., & Ward, P. J. (2023). A spatially-dependent synthetic global dataset of extreme sea level events. *Weather and Climate Extremes*, *41*, 100596. https://doi.org/10.1016/j.wace.2023.100596
Lu, Y., Seiyon Lee, B., & Doss-Gollin, J. (2025). Bayesian spatiotemporal nonstationary model quantifies robust increases in daily extreme rainfall across the Western Gulf Coast. *Environmental Research: Climate*, *4*(3), 035016. https://doi.org/10.1088/2752-5295/adf56e
Muis, S., Verlaan, M., Winsemius, H. C., Aerts, J. C. J. H., & Ward, P. J. (2016). A global reanalysis of storm surges and extreme sea levels. *Nature Communications*, *7*(1), 11969. https://doi.org/10.1038/ncomms11969
Muis, S., Apecechea, M. I., Dullaart, J., de Lima Rego, J., Madsen, K. S., Su, J., et al. (2020). A High-Resolution Global Dataset of Extreme Sea Levels, Tides, and Storm Surges, Including Future Projections. *Frontiers in Marine Science*, *7*. Retrieved from https://www.frontiersin.org/article/10.3389/fmars.2020.00263
Muis, S., Aerts, J. C. J. H., Á. Antolínez, J. A., Dullaart, J. C., Duong, T. M., Erikson, L., et al. (2023). Global Projections of Storm Surges Using High-Resolution CMIP6 Climate Models. *Earth's Future*, *11*(9), e2023EF003479. https://doi.org/10.1029/2023EF003479
Murphy, K., Fierro-Arcos, D., Rohr, T., Green, D., Novaglio, C., Baker, K., et al. (2025). Developing a Southern Ocean Marine Ecosystem Model Ensemble to Assess Climate Risks and Uncertainties. *Earth's Future*, *13*(3), e2024EF004849. https://doi.org/10.1029/2024EF004849
Nimura, M., Nishida, S., Kawasaki, K., Murakami, T., & Shimokawa, S. (2020). Storm Surge Inundation Analysis with Consideration of Building Shape and Layout at Ise Bay by Maximum Potential Typhoon. *Journal of Marine Science and Engineering*, *8*(12), 1024. https://doi.org/10.3390/jmse8121024

OCHA. (2025). Humanitarian Datasets | Find Crisis Data | HDX. Retrieved December 25, 2025, from https://data.humdata.org/dataset/
Shimura, T., Pringle, W. J., Mori, N., Miyashita, T., & Yoshida, K. (2022). Seamless Projections of Global Storm Surge and Ocean Waves Under a Warming Climate. *Geophysical Research Letters*, *49*(6), e2021GL097427. https://doi.org/10.1029/2021GL097427
Sprintall, J., Nagura, M., Hermes, J., Roxy, M. K., McPhaden, M. J., Rao, E. P. R., et al. (2024). COVID Impacts Cause Critical Gaps in the Indian Ocean Observing System. *Bulletin of the American Meteorological Society*, *105*(3), E725–E741. https://doi.org/10.1175/BAMS-D-22-0270.1
Tadesse, M. G., & Wahl, T. (2021). A database of global storm surge reconstructions. *Scientific Data*, *8*(1), 125. https://doi.org/10.1038/s41597-021-00906-x
Tadesse, M. G., Wahl, T., Rashid, M. M., Dangendorf, S., Rodríguez-Enríquez, A., & Talke, S. A. (2022). Long-term trends in storm surge climate derived from an ensemble of global surge reconstructions. *Scientific Reports*, *12*(1), 13307. https://doi.org/10.1038/s41598-022-17099-x
Takagi, H., Anh, L. T., Islam, R., & Hossain, T. T. (2023). Progress of disaster mitigation against tropical cyclones and storm surges: a comparative study of Bangladesh, Vietnam, and Japan. *Coastal Engineering Journal*, *65*(1), 39–53. https://doi.org/10.1080/21664250.2022.2100179
Tariq Masood Ali Khan, O. P. S., Md. Sazedur Rahman. (2000). Recent Sea Level and Sea Surface Temperature Trends Along the Bangladesh Coast in Relation to the Frequency of Intense Cyclones. *Marine Geodesy*, *23*(2), 103–116. https://doi.org/10.1080/01490410050030670
Tiggeloven, T., de Moel, H., Winsemius, H. C., Eilander, D., Erkens, G., Gebremedhin, E., et al. (2020). Global-scale benefit–cost analysis of coastal flood adaptation to different flood risk drivers using structural measures. *Natural Hazards and Earth System Sciences*, *20*(4), 1025–1044. https://doi.org/10.5194/nhess-20-1025-2020
Titley, H. A., Yamaguchi, M., & Magnusson, L. (2019). Current and potential use of ensemble forecasts in operational TC forecasting: results from a global forecaster survey. *Tropical Cyclone Research and Review*, *8*(3), 166–180. https://doi.org/10.1016/j.tcrr.2019.10.005
Vousdoukas, M. I., Mentaschi, L., Voukouvalas, E., Verlaan, M., Jevrejeva, S., Jackson, L. P., & Feyen, L. (2018). Global probabilistic projections of extreme sea levels show intensification of coastal flood hazard. *Nature Communications*, *9*(1), 2360. https://doi.org/10.1038/s41467-018-04692-w
Wahl, T., Haigh, I. D., Nicholls, R. J., Arns, A., Dangendorf, S., Hinkel, J., & Slangen, A. B. A. (2017). Understanding extreme sea levels for broad-scale coastal impact and adaptation analysis. *Nature Communications*, *8*(1), 16075. https://doi.org/10.1038/ncomms16075
Yamaguchi, M., Vitart, F., Lang, S. T. K., Magnusson, L., Elsberry, R. L., Elliott, G., et al. (2015). Global Distribution of the Skill of Tropical Cyclone Activity Forecasts on Short- to Medium-Range Time Scales. *Weather and Forecasting*, *30*(6), 1695–1709. https://doi.org/10.1175/WAF-D-14-00136.1